



ELSEVIER

16 September 1999

PHYSICS LETTERS B

Physics Letters B 462 (1999) 453–461

## Evidence for two pseudoscalar states in the 1.4–1.5 GeV mass region

OBELIX collaboration

C. Cicalo<sup>a</sup>, A. De Falco<sup>a</sup>, A. Masoni<sup>a</sup>, S. Mauro<sup>a</sup>, G. Puddu<sup>a</sup>, S. Serci<sup>a</sup>,  
P. Temnikov<sup>a,1</sup>, G. Usai<sup>a</sup>, A. Bertin<sup>b</sup>, M. Bruschi<sup>b</sup>, M. Capponi<sup>b</sup>, S. De Castro<sup>b</sup>,  
R. Dona<sup>b</sup>, D. Galli<sup>b</sup>, B. Giacobbe<sup>b</sup>, U. Marconi<sup>b</sup>, I. Massa<sup>b</sup>, M. Piccinini<sup>b</sup>,  
M. Poli<sup>b,2</sup>, N. Semprini Cesari<sup>b</sup>, R. Spighi<sup>b</sup>, V. Vagnoni<sup>b</sup>, S. Vecchi<sup>b</sup>, M. Villa<sup>b</sup>,  
A. Vitale<sup>b</sup>, A. Zoccoli<sup>b</sup>, A. Bianconi<sup>c</sup>, G. Bonomi<sup>c</sup>, E. Lodi Rizzini<sup>c</sup>,  
L. Venturelli<sup>c</sup>, A. Zenoni<sup>c</sup>, O.E. Gorchakov<sup>d</sup>, S.N. Prakhov<sup>d</sup>,  
A.M. Rozhdestvensky<sup>d</sup>, V.I. Tretyak<sup>d</sup>, P. Gianotti<sup>e</sup>, C. Guaraldo<sup>e</sup>, A. Lanaro<sup>e</sup>,  
V. Lucherini<sup>e</sup>, C. Petrascu<sup>e</sup>, V. Ableev<sup>f,3</sup>, M. Lombardi<sup>f</sup>, G. Vedovato<sup>f</sup>,  
V. Filippini<sup>g</sup>, A. Fontana<sup>g</sup>, P. Montagna<sup>g</sup>, A. Rotondi<sup>g</sup>, P. Salvini<sup>g</sup>,  
M. Agnello<sup>h,4</sup>, F. Balestra<sup>h</sup>, E. Botta<sup>h</sup>, T. Bressani<sup>h</sup>, L. Busso<sup>h</sup>, P. Cerello<sup>h</sup>,  
D. Calvo<sup>h</sup>, S. Costa<sup>h</sup>, O. Denisov<sup>h,3</sup>, D. D'Isep<sup>h</sup>, A. Feliciello<sup>h</sup>, L. Ferrero<sup>h</sup>,  
A. Filippi<sup>h</sup>, R. Garfagnini<sup>h</sup>, A. Grasso<sup>h</sup>, F. Iazzi<sup>h,4</sup>, A. Maggiore<sup>h</sup>,  
S. Marcello<sup>h</sup>, B. Minetti<sup>h,4</sup>, N. Mirfakhrai<sup>h,5</sup>, A. Panzarasa<sup>h</sup>, D. Panzieri<sup>h</sup>,  
F. Tosello<sup>h</sup>, S. Tessaro<sup>i</sup>

<sup>a</sup> Dipartimento di Fisica, Università di Cagliari and INFN, Sezione di Cagliari, Cagliari, Italy

<sup>b</sup> Dipartimento di Fisica, Università di Bologna and INFN, Sez. di Bologna, Bologna, Italy

<sup>c</sup> Dipartimento di Chimica e Fisica per l'Ingegneria e per i Materiali, Università di Brescia and INFN Sezione di Pavia, Pavia, Italy

<sup>d</sup> Joint Institute of Nuclear Research, Dubna, Moscow, Russia

<sup>e</sup> Laboratori Nazionali di Frascati dell' INFN, Frascati, Italy

<sup>f</sup> Laboratori Nazionali di Legnaro dell' INFN, Legnaro, Italy

<sup>g</sup> Dipartimento di Fisica Nucleare e Teorica, Università di Pavia and INFN, Sezione di Pavia, Pavia, Italy

<sup>h</sup> Istituto di Fisica, Università di Torino and INFN, Sez. di Torino, Torino, Italy

<sup>i</sup> Istituto di Fisica, Università di Trieste and INFN, Sez. di Trieste, Trieste, Italy

Received 20 July 1999; received in revised form 29 July 1999; accepted 29 July 1999

Editor: L. Montanet

## Abstract

A confirming evidence for two pseudoscalar states with masses  $M_1 = 1405 \pm 5$ ,  $\Gamma_1 = 50 \pm 4$  MeV/ $c^2$  and  $M_2 = 1500 \pm 10$ ,  $\Gamma_2 = 100 \pm 20$  MeV/ $c^2$  is reported. The second pseudoscalar fills the nonet and leaves the first as an outsider supporting the hypothesis for its exotic nature. © 1999 Published by Elsevier Science B.V. All rights reserved.

Since the first observation of a peak in the  $K\bar{K}\pi$  mass spectrum in  $\bar{p}p$  annihilation at rest in 1963 [1] 28 experiments for over 35 years investigated the nature of the resonant structure usually known as  $E/\nu$ .

It is now well established the presence of an axial vector:  $f_1(1420)$  and one pseudoscalar:  $\eta(1440)$ . The possible splitting in two states of the  $\eta(1440)$  is not established yet (see PDG [2]. For a detailed review see Ref. [3]).

The presence of a second pseudoscalar state assumes considerable significance. It would fill the pseudoscalar nonet leaving out the lower mass pseudoscalar:  $\eta(1400)$  and would certainly support the hypothesis of its non  $q\bar{q}$  nature.

The first experiment resolving the two pseudoscalars was MARK III, which reported one  $0^{-+}$  at  $1416 \pm 8$  MeV decaying to  $a_0\pi$  and another pseudoscalar at  $1490^{+14}_{-8}$  MeV decaying to  $K^*\bar{K}$  [4]. This result was confirmed by DM2 but in this case the masses were  $1421 \pm 14$  and  $1459 \pm 5$  MeV and the decay modes for the two pseudoscalar were inverted with respect to the MARK III result. Also in  $\pi^-p \rightarrow \bar{K}K\pi n$  peripheral collision two resonant states were reported [5]. In this case only the parameters of the lower mass pseudoscalar ( $M = 1407 \pm 3$  MeV  $\Gamma = 75 \pm 6$  MeV) were given [6–8].

More recently two pseudoscalars were observed again in  $\bar{p}p \rightarrow K^\pm K_L^0 \pi^\mp \pi\pi$  annihilation at rest by

the Obelix experiment [9,10]. The best evidence came from the liquid hydrogen data [9]. In this case the  $\bar{p}p$  annihilation proceeds mainly from  $S$  – states enhancing the pseudoscalars contribution (see Ref. [9]).

In this paper we report a new measurement of the channel  $\bar{p}p \rightarrow K^\pm K_S^0 \pi^\mp \pi^+ \pi^-$  with  $K_S^0 \rightarrow \pi^+ \pi^-$ . The final state is the same but the advantage with respect to the data of Ref. [9] is that no missing particle is present and contamination from other channels (see below) is negligible (it was around 20% in ref [9]). Moreover a new analysis approach has been adopted with energy dependent widths in order to describe the threshold behaviour of the  $K^*\bar{K}$  decay.

The experiment was performed at the Low Energy Antiproton Ring (LEAR) at CERN, using the OBELIX spectrometer. The apparatus can be regarded as an ensemble of four subdetectors having cylindrical geometry (a detailed description can be found in Ref. [11]), arranged between the poles of the Open Axial Filed Magnet (OAFM) of CERN. In the present analysis only TOF (Time Of Flight) and drift chamber (JDC) subsystems were exploited.

Antiprotons with a momentum of 200 MeV/ $c$  were stopped in a liquid hydrogen target. For this measurement a two cm diameter target together with a silicon detector system were envisaged in order to improve vertex constraints. The trigger based on the Time Of Flight system selected six prong annihilations requiring 6 hits in the inner TOF barrel and at least 3 hits in the external one.

Six tracks were reconstructed by JDC with zero total charge, all pointing to the target region. The events were selected on the following basis: identification of one kaon and five pions in the final state by means of  $dE/dx$  and Time-Of-Flight; 5C kinematical fit for the channel  $K^\pm K_S^0 \pi^\mp \pi^+ \pi^-$  (with  $K_S^0 \rightarrow \pi^+ \pi^-$ ) with 90% CL. The particle identification

<sup>1</sup> on leave of absence from Institute for Nuclear Research and Nuclear Energy, Sofia, Bulgaria

<sup>2</sup> Dipartimento di Energetica “Sergio Stecco”, Università di Firenze, Firenze, Italy

<sup>3</sup> on leave of absence from Joint Institute of Nuclear Research, Dubna, Moscow, Russia

<sup>4</sup> Politecnico di Torino and INFN, Sez. di Torino, Torino, Italy

<sup>5</sup> Shahid Beheshti University, Teheran, Iran

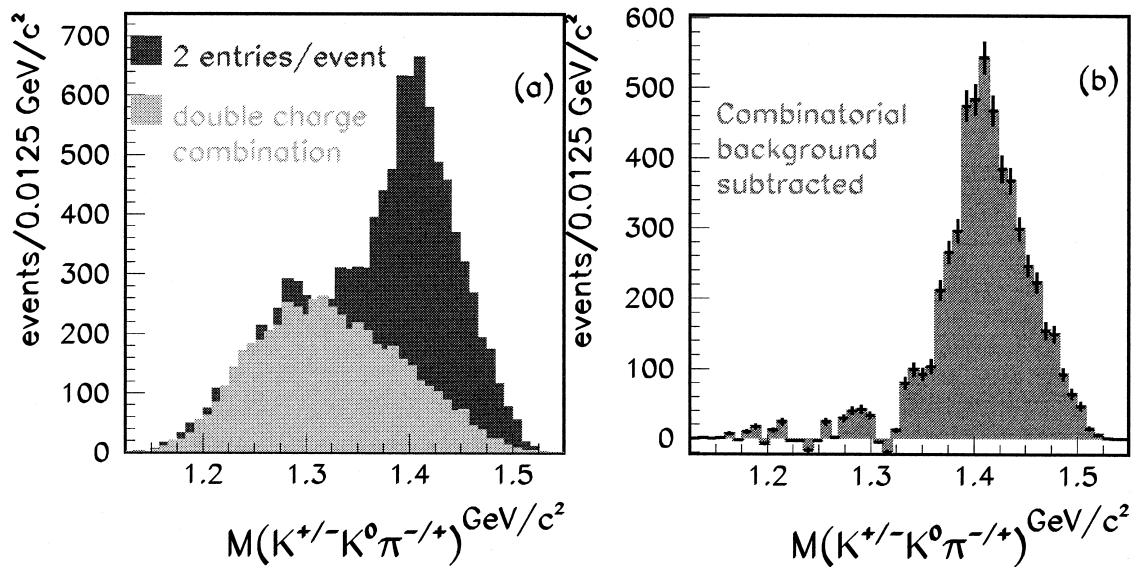


Fig. 1. a) Invariant mass  $K\bar{K}\pi$  and double charge combination; b) mass distribution without combinatorial background

selection was tuned in such a way to obtain a flat efficiency (80%) as a function of momentum and a rejection on pions  $> 99\%$ . With this selections the background from other competing channels results negligible ( $< 1\%$ , as checked by Monte Carlo Simulation). In the end a total of 5400 events were

retained. Fig. 1(a) shows the  $K^\pm K_S^0 \pi^\mp$  invariant mass (two entries/event) together with the double charge combination. The subtraction of the two histograms produces a combinatorial background-free distribution which is shown in Fig. 1(b). The prominent  $E/\nu$  signal stems clearly in the histogram.

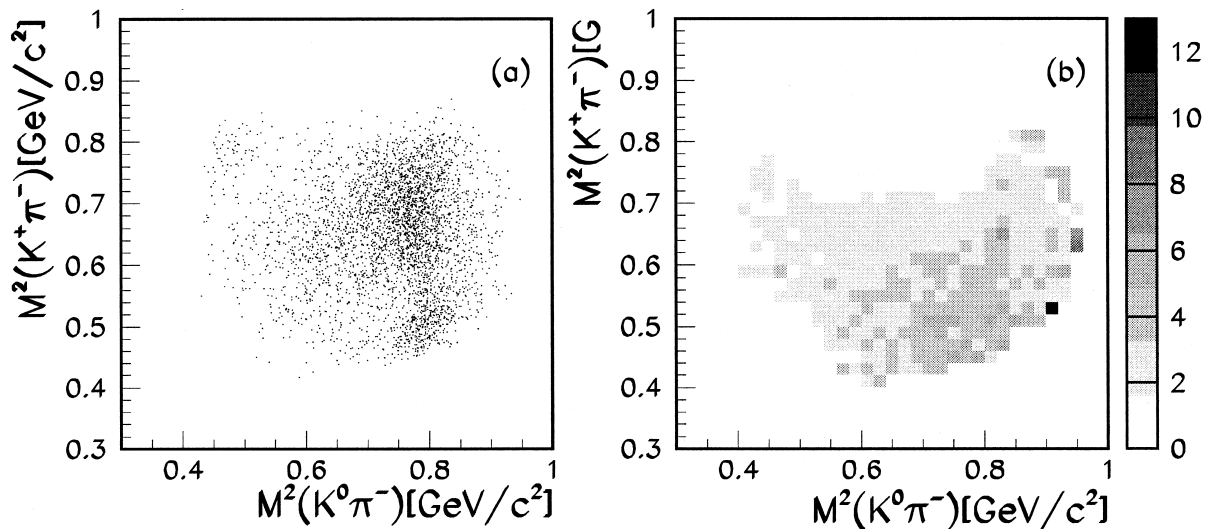


Fig. 2. a) experimental Dalitz plot; b) acceptance Dalitz plot

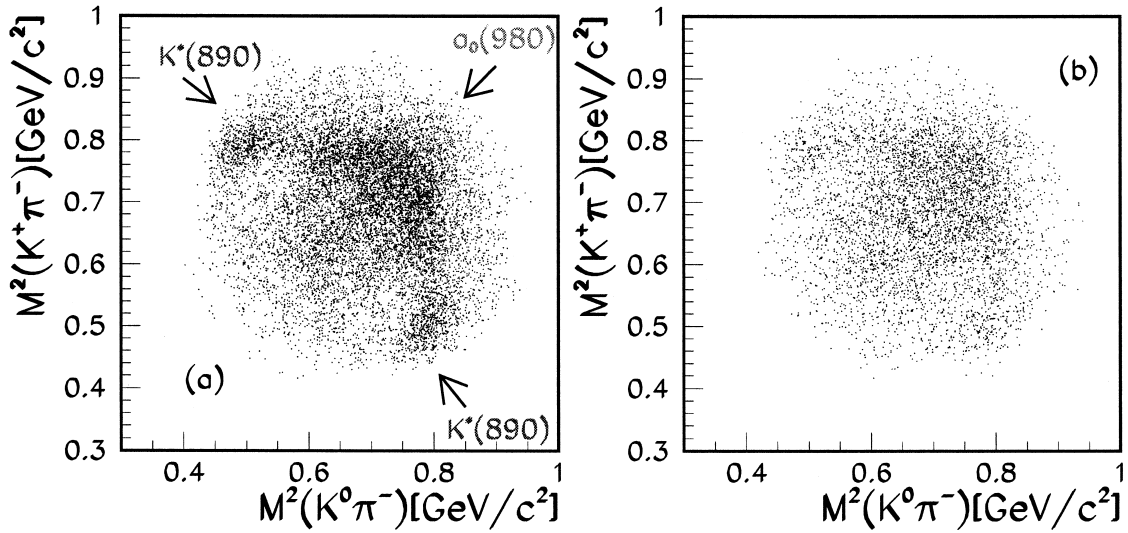


Fig. 3. a) 6 prong folded Dalitz plot; b) 4 prong folded Dalitz plot

The  $E/\iota$  decay Dalitz plot is shown in Fig. 2(a) for  $1380 < m(K\bar{K}\pi) < 1500 \text{ MeV}/c^2$ . The structure due to the  $K^{*0}$  is clearly seen. The experimental apparatus has a detection threshold at about 180 MeV/c for charged kaons, which has the effect to suppress the high  $K^0\pi^\mp$  invariant masses, cutting

the  $K^{*\pm}$  signal. On the other hand, above that threshold acceptance is quite good as shown in the (Monte Carlo) acceptance Dalitz plot of Fig. 2(b).

We can reconstruct the missing part of the Dalitz plot folding the ‘‘good’’ part along the diagonal. The result is shown in Fig. 3(a). The typical structure

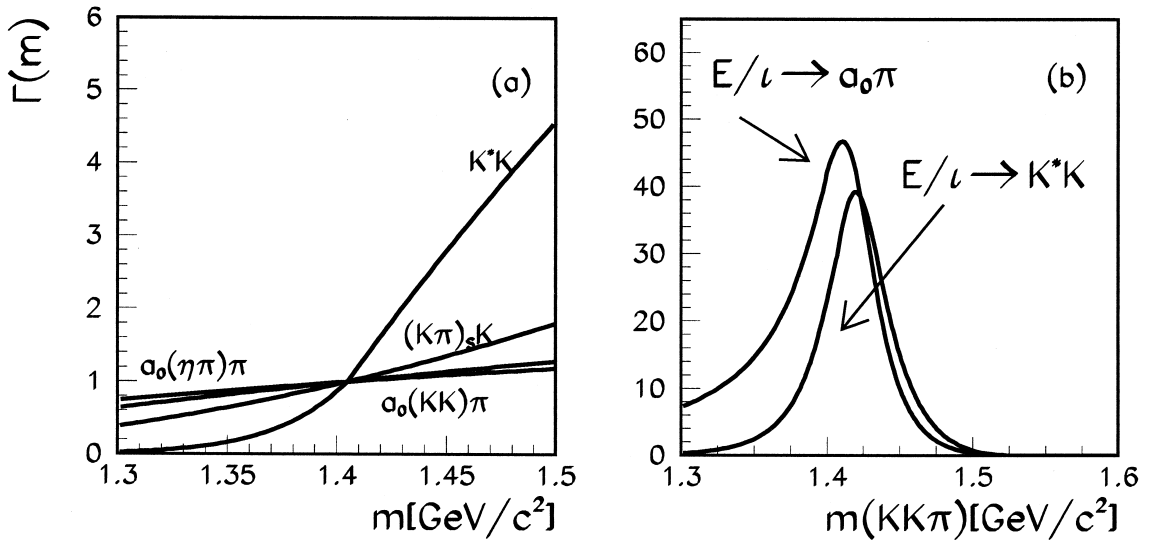


Fig. 4. a) Partial widths as a function of energy; b) cross sections for  $E/\iota \rightarrow a_0\pi, K^*\bar{K}$

related to  $K^*$  coming from a  $0^-$  state is evident. In Fig. 3(b) we show for comparison the 4 prong Dalitz plot of Ref. [9]. Because of the higher statistics, the background suppression and the improved vertex definition, the structures in the new data are definitely better resolved and cleaner.

The spin-parity analysis was performed within the isobar model. For the process  $\bar{p}p \rightarrow E/\iota(\pi\pi)$ ,  $E/\iota \rightarrow K^*\bar{K}$ , for instance, amplitude is parametrized in the following way [12,9] (ignoring isospin decompositions and the  $\pi\pi$  parametrization):

$$A \propto BW(E/\iota) BW(K^*) T_{K^*\bar{K}}. \quad (1)$$

Here  $T$  is a spin component of the amplitude calculated with the helicity formalism, while  $BW$  is a Breit-Wigner function.  $E/\iota$  can have different decay modes ( $a_0\pi, K^*\bar{K}, K\bar{K}\pi, \dots$ ), so that the total width is the sum of the partial widths,

$$\Gamma_{E/\iota} = \Gamma_{a_0\pi}(\sqrt{s}) + \Gamma_{K^*\bar{K}}(\sqrt{s}) + \Gamma_{K\bar{K}\pi}(\sqrt{s}) + \Gamma_{\text{else}}(\sqrt{s}), \quad (2)$$

where  $\sqrt{s} = m_{K\bar{K}\pi}$ ,  $\Gamma_{\text{else}}(\sqrt{s})$  is the total decay width to unobserved final states, such as  $\eta\pi\pi$  or  $\eta'\pi\pi$  [3].

The single partial widths are given by the integral of the square module of the  $E/\iota$  decay amplitude over the available phase space. For instance, considering the process  $E/\iota \rightarrow K^*\bar{K}$ , we have

$$\Gamma_{K^*\bar{K}}(\sqrt{s}) = g_{K^*\bar{K}}^2 \int_{\sqrt{s}} |A_{E/\iota \rightarrow K^*\bar{K}}|^2 d\Omega, \quad (3)$$

where  $g_{K^*\bar{K}}$  is a coupling constant while  $d\Omega$  is the available phase space. The decay amplitude has the

form  $A_{E/\iota \rightarrow K^*\bar{K}} = BW(K^*) \cdot T_{K^*\bar{K}}$ . In Fig. 4(a) we present the partial widths as function of  $m_{K\bar{K}\pi}$  (normalized at  $m_{K\bar{K}\pi} = 1405 \text{ MeV}/c^2$ ). We observe that, while all other widths are smoothly constant the width for the  $K^*\bar{K}$  decay exhibits a threshold effect and a fast raise due to the spin structure.

The  $E/\iota$  production rate has the form

$$d\sigma(\sqrt{s}) \propto |BW(E/\iota)|^2 \int_{\sqrt{s}} |A_{E/\iota \rightarrow K^*\bar{K}}|^2 d\Omega = \frac{\Gamma_{E/\iota \rightarrow K^*\bar{K}}}{(m_{E/\iota}^2 - m_{K\bar{K}\pi}^2)^2 + m_{E/\iota}^2 \Gamma_{\text{tot}}^2(m_{K\bar{K}\pi})}. \quad (4)$$

The normalized production rates for  $E/\iota \rightarrow a_0\pi$ , and  $E/\iota \rightarrow K^*\bar{K}$  are shown in Fig. 4(b) (with phase space limitations and assuming their equality). A clear asymmetry in the  $K^*\bar{K}$  distribution is seen: there is a shift forward for the peak position. In our case of  $\bar{p}p$  annihilations at rest, the  $E/\iota$  production suffers a phase space limitation. The  $K^*\bar{K}$  production rate peaks at a higher mass than  $a_0\pi$ . It has the effect to suppress more selectively the  $K^*\bar{K}$  decay mode with respect to other processes such as  $a_0\pi$  or  $K\bar{K}\pi$ .

We have first performed a series of fits including only one pseudoscalar, varying its mass in order to optimize the log-likelihood value. The minimum is found at about 1420–1425  $\text{MeV}/c^2$  (see Fig. 5(a)).

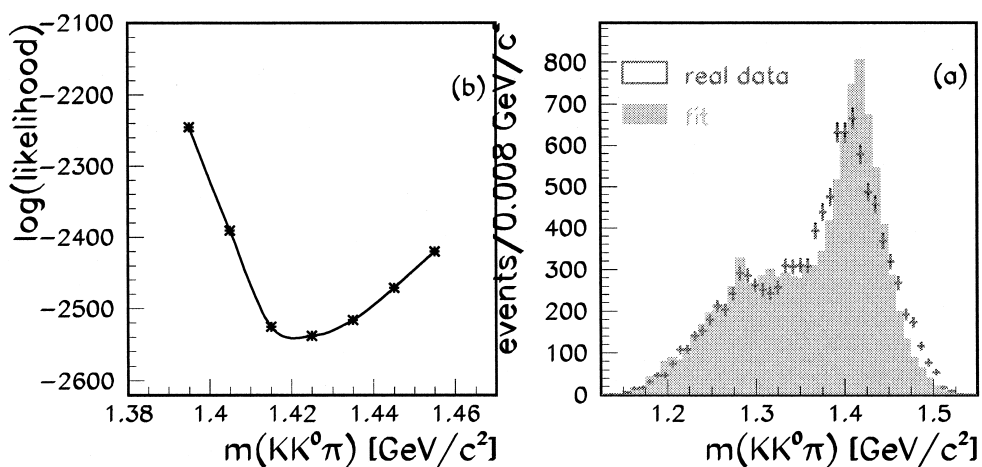


Fig. 5. Fit with one pseudoscalar: a)  $\log(L)$  as a function of  $m_{K\bar{K}\pi}$ ; b)  $K\bar{K}\pi$  invariant mass (errors) and the fit result (shaded)

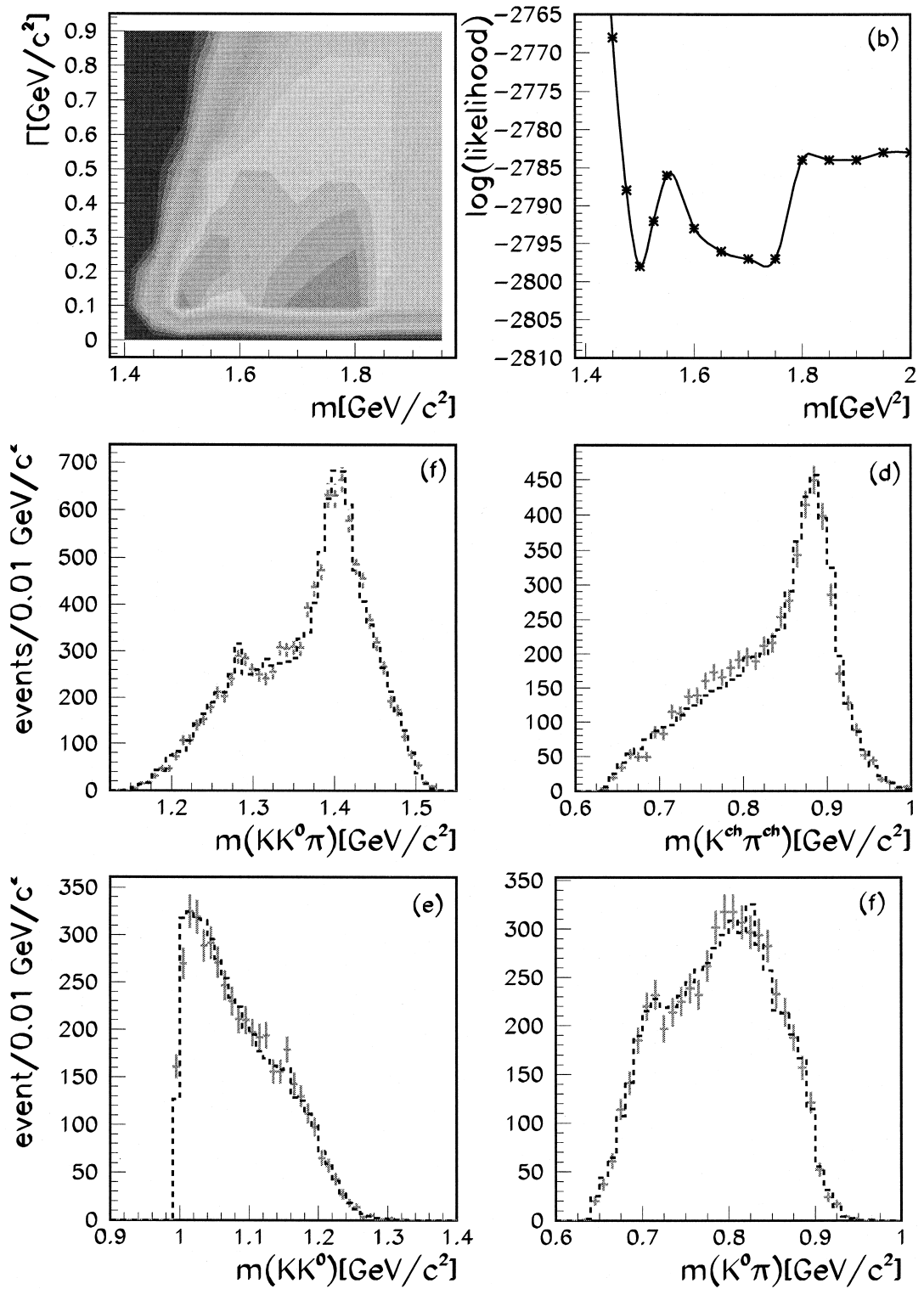


Table 1  
Partial widths (normalized to the  $K\bar{K}\pi$  decay modes)

		$\Gamma_{K\bar{K}\pi}$	$\Gamma_{a_0\pi}$	$\Gamma_{K^*\bar{K}}$
Solution (A)	$\eta(1440)$	1	$0.1 \pm 0.01$	$0.8 \pm 0.02$
$L = 2550; \chi^2 = 3.0$	–	–	–	–
Solution (B)	$\eta(1400)$	1	$0.2 \pm 0.01$	$0.4 \pm 0.01$
$L = 2800; \chi^2 = 1.4$	$\eta(1500)$	1	$0.1 \pm 0.01$	$4 \pm 0.2$
Solution (C)	$\eta(1400)$	1	$0.1 \pm 0.01$	$0.8 \pm 0.02$
$L = 2800; \chi^2 = 1.4$	$\eta(1700\text{--}1800)$	1	$0.1 \pm 0.1$	$2 \pm 0.1$

In Fig. 5(b) the  $K\bar{K}\pi$  invariant mass (histogram with errors) is shown together with the fit result (shaded histogram). The fit is clearly unsatisfactory: we are not able to describe the  $E/\iota$  structure by means of one pseudoscalar state only. The  $\chi^2$  evaluated over a set of one-dimensional histograms is greater than 3.

In a second attempt we included two pseudoscalar states. In order to find the optimal mass and width of the two states, we fixed mass and width of the first one and performed a likelihood scan varying mass and width of the second one. The procedure was repeated for several values of the mass of the first state at steps of 10 MeV/ $c^2$ : 1395, 1405, 1415, 1425 MeV/ $c^2$ . The optimal mass of the first state is found at about 1405 MeV/ $c^2$ . In Fig. 6(a) we show the likelihood scan as a function of mass and width of the second state when the mass of the first one is 1405 MeV/ $c^2$ . Fig. 6(b) shows the projection referred to the mass scan. Two equivalent minima are found. They lead to two different solutions each one requiring two pseudoscalar states. For both there is a substantial improvement with respect to the single pseudoscalar hypothesis:  $\chi^2 \sim 1.4$ , and  $\log(L) \sim -2800$  ( $\log(L(20^{-+})) - \log(L(10^{-+})) \sim 250$ ). The data description is shown in Fig. 4(c–f). The partial widths of each state (normalized to the  $K\bar{K}\pi$  one) for each solutions are shown in Table 1.

The first solution requires a  $\eta(1400)$  with  $m = 1405 \pm 5$ ,  $\Gamma = 50 \pm 4$  MeV/ $c^2$  decaying dominantly to  $K\bar{K}\pi$ , and a  $\eta(1500)$  with  $m = 1500 \pm 10$ ,  $\Gamma = 100 \pm 20$  MeV/ $c^2$  decaying dominantly to

$K^*\bar{K}$ . That solution is compatible with what we had found in the 4 prong data [9].

The second solution requires a  $\eta(1400)$  with the same mass and width and a  $\eta(1700\text{--}1800)$  with mass (1700 to 1800 MeV/ $c^2$ ) and width (100 to 400 MeV/ $c^2$ ). In this case the  $\eta(1400)$  is more coupled to  $K^*\bar{K}$ , while the higher mass state is less coupled to  $K^*\bar{K}$ .

The main results of the fit is that the hypothesis of one pseudoscalar is rejected and two pseudoscalar are definitely required. The improvement in  $\log(L)$  (250 units) and in the  $\chi^2$  evaluated on one dimensional histograms ( $\chi^2 \sim 1.4$  versus  $\chi^2 \sim 3.0$ ) provide a clean evidence for that.

Concerning the two possible solutions (B and C on Table 2) they are equivalent from the fitting point of view. Nevertheless there are several arguments to choose solution B and reject solution C. As a matter of fact, while for solution B mass and width of the second pseudoscalar agree well both with the previous Obelix results [9,10] and the data reported by MARKIII and DM2 [4,5], in solution C the second pseudoscalar appears at a definitely higher and not well defined mass and with a larger width. But even more important are the results on the decay modes. Practically all experiments agree on the following picture: there is a low mass (1400–1420 MeV) pseudoscalar ( $\eta_L$ ) with  $a_0\pi$  or direct  $\eta\pi\pi$ ,  $K\bar{K}\pi$  decay modes [4,9,10,6,7,13–18,22]; a higher mass pseudoscalar ( $\eta_H$ ) is reported at 1500 MeV only in  $K\bar{K}\pi$  experiments decaying to  $K^*\bar{K}$ .

Fig. 6. Fit with two pseudoscalars: a)  $\log(L)$  as a function of mass and width of second pseudoscalar (the mass and width of the first one are fixed at 1405 and 50 MeV/ $c^2$ , respectively); b)  $\log(L)$  as a function of mass of second pseudoscalar; c–f) Data description of the fit with two pseudoscalar states

Table 2  
S- and P-wave fractions for the different isobar contributions

	Solution B	Solution C
S-wave/Signal	89%	89%
$\eta_{\text{low}}/S\text{-wave}$	$77 \pm 5 \%$	$63 \pm 5 \%$
$\eta_{\text{high}}/S\text{-wave}$	$23 \pm 3 \%$	$37 \pm 7 \%$
P-wave/Signal	11%	11 %
$f_1(1285)/P\text{-wave}$	$21 \pm 22 \%$	$21 \pm 3 \%$
$f_1(1425)/P\text{-wave}$	$79 \pm 22 \%$	$79 \pm 3 \%$
Background/Signal	5%	5%

This *scenario* perfectly agrees with solution B but it is not compatible with solution C. According to solution C the  $K^* \bar{K}$  decay mode should have been observed also for  $\eta_L$  and, even more,  $\eta_H$  should have been seen in  $\eta\pi\pi$  experiments also.

In conclusion we can now support a consistent evidence for the presence of two pseudoscalars in the mass region between 1400 and 1500 MeV. One of them stays surely out the available slots in the SU(3) nonet. The  $\eta(1295)$  is commonly accepted as the  $n\bar{n}$  member of the excited pseudoscalar nonet [2]. According to Ref. [19] the  $s\bar{s}$  member of the  $0^{-+}$  excited nonet should have a large  $K^* \bar{K}$  coupling and a width around 100 MeV. This matches well with  $\eta_H$  leaving the  $\eta_L$  as the outsider candidate. Moreover, following Ref. [20,21] from the  $J/\psi$  radiative decay production rates is possible to extract the  $\eta_L$  coupling to gluons which results very close to one:

$$b(\eta_L \rightarrow gg) = 0.9 \pm 0.2 \quad (5)$$

Summarizing, the following arguments are in favor of a large coupling to gluons:

- a) being out of the  $0^{-+}$  excited nonet;
- b) the result (5) from  $J/\psi$  radiative decay [21];
- c) the strong contribution to direct  $K\bar{K}\pi$  and  $\eta\pi\pi$  decay (see Table 1 and Ref. [9,10] for  $K\bar{K}\pi$  and Ref. [16,18,17] for  $\eta\pi\pi$ );
- d) the sizeable  $\eta'\pi\pi$  branching ratio [23];
- e) the suppression in  $\gamma\gamma$  collisions [24–27].

As shown by the points a)–e) above there is a wide, consistent, experimental evidence, furtherly supported by the latest Obelix results, indicating the fulfillment of gluonium requirements.

However, still remains to be understood the mass difference with respect to Lattice Calculations [28,29]

which predict the  $0^{-+}$  glueball at a mass above 2 GeV.

According to Ref. [21] this discrepancy between experimental data and theory can be the signal of dynamics beyond quenched lattice gauge theory at work in the  $0^{-+}$  sector, or lead to an even more exotic interpretation of  $\eta_L$  in terms of gluino-gluino bound state [21,30,31].

## References

- [1] R. Armenteros et al., Proc. of the Siena Int. Conf. on Elementary Particles 1 (1963) 287.
- [2] R.M. Barnett et al., Review of particle properties, Europ. Phys. Journal C3 (1998)
- [3] Proc. LEAP98 Conference, to be published on Nucl. Phys. B Proc. Int. Conference on Low Energy Antiprotons.
- [4] MARKIII Collaboration, Z. Bai et al., Phys. Rev. Lett. 65 (1990) 2507.
- [5] DM2 Collaboration, J.E. Augustin et al., Phys. Rev. D46 (1992) 1951.
- [6] A. Birman et al., Phys. Rev. Lett. 61 (1988) 1557.
- [7] Boehnlein et al., Nucl. Phys. B21 proc. suppl. (1991)
- [8] S. Chung, Proc. VI International Conference on Hadron Spectroscopy, M.C. Birse, G.D. Lafferty, J.A. McGovern Editors, World Scientific (1996)
- [9] Obelix Collaboration, A. Bertin et al., Phys. Lett. B 361 (1995) 187.
- [10] Obelix Collaboration, A. Bertin et al., Phys. Lett. B 400 (1997) 226.
- [11] Obelix Collaboration, A. Adamo et al., Sov. J. Nucl. Phys. 55 (1992) 1732.
- [12] S.U. Chung et al., Ann. Physik 4 (1995) 404.
- [13] M.G. Rath et al., Phys. Rev. D40 (1989) 693.
- [14] A. Ando et al., Phys. Rev. Lett. 57 (1986) 1296.
- [15] S. Fukui et al., Phys. Lett. B267 (1991) 293.
- [16] Crystal Barrel Collaboration, C. Amsler et al., Phys. Lett. B358 (1995) 389.



- [17] Alde et al., *Yad. Fiz.* (1997)
- [18] Crystal Barrel Collaboration, A. Abele et al., *Phys. Lett. B* 514 (1998) 45.
- [19] T. Barnes, F.E. Close, P. Page, E. Swanson, *Phys. Rev. D* 55 (1997) 4157.
- [20] M.B. Cakir, G.R. Farrar, *Phys. Rev. D* 50 (1994) 3268.
- [21] F.E. Close, G.R. Farrar, Z. Li, *Phys. Rev. D* 55 (1997) 5749.
- [22] C. Amsler, *Rev. Mod. Phys.* 70 (1998) 1293.
- [23] N. Djaoshvili, L. Montanet, *Nucl. Phys. B (Proc. Suppl.)* 64 (1998) 199.
- [24] G. Gidal et al., *Phys. Rev. Lett.* 59 (1987) 2012, 2016.
- [25] H. Aihara et al., *Phys. Rev. D* 38 (1988) 1.
- [26] P. Hill et al., *Z. Phys. C* 42 (1989) 355.
- [27] H.J. Behrend et al., *Z. Phys. C* 42 (1989) 367.
- [28] C. Michael, *Proc. LEAP98 Conference*, to be published in *Nucl. Phys. B*
- [29] A. Szczpaniak, E.S. Swanson, C.R. Ji, S.R. Cotanch, *Phys. Rev. Lett.* 76 2011.
- [30] G.R. Farrar, *Phys. Rev. D* 51 (1995) 3904.
- [31] G.R. Farrar, *Phys. Rev. Lett.* (1996) 4111.